Ni^{57} should have the configuration $p_{3/2}$ and that of Co^{57} $f_{7/2}$. The present experiments are in agreement with this prediction, since there is no positron decay to the ground state. Since the positron transition to the 1.375-Mev state of Co^{57} is allowed, the configuration of this state is probably $p_{3/2}$. In addition, since the $p_{3/2}$ and $f_{5/2}$ states have nearly the same energy in this region, it is probable that the state at 1.50 Mev has the configuration $f_{5/2}$.

The authors are indebted to Dr. M. B. Sampson and the cyclotron crew for making the bombardments, to Mr. Arthur Lessor for making the chemical separations, and to Dr. R. G. Wilkinson and Mr. Harvey Israel for help with the investigation of the positron spectrum.

PHYSICAL REVIEW VOLUME 83, NUMBER 5 SEPTEMBER 1, 1951

Z Dependence and Angular Distribution of Bremsstrahlung from 17-Mev Electrons*

L. H. Lanzl† and A. O. Hanson
Department of Physics, University of Illinois, Urbana, Illinois
(Received April 16, 1951)

The relative bremsstrahlung cross section for the upper portion of the spectrum as a function of Z, for 17-Mev electrons from a 22-Mev betatron, has been measured. The radiation was detected by means of the $Cu^{63}(\gamma,n)$ induced activity, which has a 10.9-Mev threshold. The effect of atomic screening is small for the quantum energies to which this detector responds, but was taken into account. The results are in agreement with the Bethe-Heitler theory for electron-nuclear interactions within 1 percent. Electron-electron interactions give 0.75 times the intensity for electron-proton interactions, as measured with a copper detector.

The total cross section for radiative energy loss of electrons has been measured with an ionization chamber. The experimental Z dependence of the relative cross section indicates that the yield from gold for a given $N(Z^2+Z)$ is somewhat less than that from low Z elements. This discrepancy might be accounted for by improved corrections for screening, and by more accurate consideration of the radiation produced by electron-electron impacts. Rough measurements of the absolute cross section are in agreement with the Bethe-Heitler theory.

The intrinsic angular distribution of bremsstrahlung, produced in a small amount of cellophane and air, was measured by film and ion chamber, and was found to fit a $1/[1+(E\theta/\mu)^2]^2$ distribution. The angular distribution was measured with three detectors, for one Be and several Au targets. The results are in agreement with calculations in which the above intrinsic distribution and Molière's multiple scattering theory are used.

The central intensity of bremsstrahlung as a function of target thickness, measured with a small ion chamber, is in approximate agreement with a calculation in which the energy loss of the primary electrons has been taken into account.

INTRODUCTION

THE amount of energy radiated during the passage of electrons through matter has been studied by two methods: (1) by measuring the electron energy before and after passage through a given material, the difference in energy being a measure of the total energy loss, which is caused mainly by ionization or excitation, and by radiation; (2) by measuring the bremsstrahlung itself. This latter method was the one used in the experiments to be presented in this paper, the electron source being a betatron.

Blackett[1] and Anderson and Neddermeyer[2] performed cloud-chamber experiments in which the total energy loss of cosmic-ray electrons in lead was determined by the first method. Some typical results obtained by Anderson and Neddermeyer near 30 Mev were about 16 percent lower than predicted by the Bethe-Heitler theory.[3] Although a number of experiments on energy loss have been performed with β-rays, those at energies below about 9 Mev are of little use in a direct check of the theory because of the multiple scattering which the electrons undergo.[4] Results for β-rays of 9 to 13.5 Mev indicate energy losses of about 1.4 times the theoretical values.[5–7]

The electrostatic generator was used by Ivanov *et al.*[8] for calorimetric measurements of the radiation output from a thick lead target, with results lower than given by the Bethe-Heitler theory for bremsstrahlung production and by that of Bloch[9] for collision loss. Buechner and Van de Graaff[10] found experimentally, with 2-Mev electrons from a Van de Graaff generator, and by using a very thick calorimeter, that no energy is carried away by any means other than radiation, e.g., in the form of neutrinos.

Van Atta, Petrauskas, and Myers[11] measured the

* This work was assisted in part by the joint program of the ONR and AEC.

† Now at Argonne Cancer Research Hospital, University of Chicago, Chicago, Illinois.

[1] P. M. S. Blackett, Proc. Roy. Soc. (London) **165**, 11 (1938).

[2] C. D. Anderson and S. H. Neddermeyer, Phys. Rev. **50**, 263 (1936).

[3] H. Bethe and W. Heitler, Proc. Roy. Soc. (London) **146**, 83 (1934); see also H. Bethe, Proc. Cambridge Phil. Soc. **30**, 524 (1934).

[4] M. M. Slawsky and H. R. Crane, Phys. Rev. **56**, 1203 (1939).

[5] W. A. Fowler and J. Oppenheimer, Phys. Rev. **54**, 320 (1938).

[6] A. J. Ruhlig and H. R. Crane, Phys. Rev. **53**, 618 (1938).

[7] J. J. Turin and H. R. Crane, Phys. Rev. **52**, 63 (1937).

[8] Ivanov, Walther, Sinelnikov, Taranov, and Abramovich, J. Phys. (U.S.S.R.) **4**, 319 (1941).

[9] F. Bloch, Z. Physik **81**, 363 (1933).

[10] W. W. Buechner and R. J. Van de Graaff, Phys. Rev. **70**, 174 (1946).

[11] Van Atta, Petrauskas, and Myers, Am. J. Roentgenol. Radium Therapy **50**, 803 (1943).

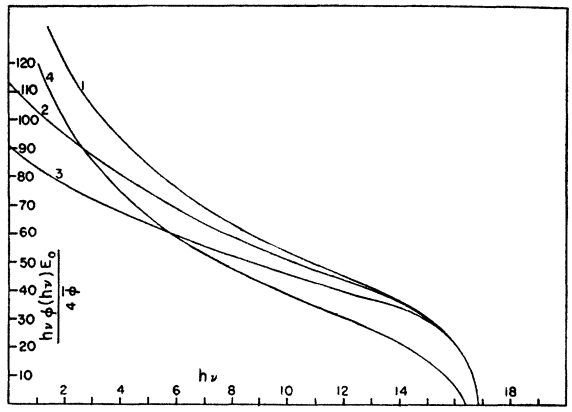

FIG. 1. Bremsstrahlung intensity distribution as a function of quantum energy, $h\nu$, from 16.93-Mev monokinetic electrons. The ordinate is in units of $E_0/4\bar{\phi}$, where $\bar{\phi}=Z^2r_0^2/137$, and E_0=total electron energy in Mev. Curve 1: Unscreened nucleus. Curve 2: Beryllium. Curve 3: Gold. Curve 40: Bremsstrahlung from electron-electron collisions.

angular distribution and efficiency of production of bremsstrahlung in a $\frac{1}{32}$-in. gold target, by monokinetic electrons of incident energies between 0.7 and 2.5 Mev, using a small ion chamber with air-equivalent wall material. The efficiency of bremsstrahlung production, when compared to the Bethe-Heitler theory, was found to be 12 percent lower at 0.9 Mev, 4 percent higher at 1.63 Mev, and 20 percent higher at 2.35 Mev.

Korsunsky *et al.*[12] investigated the Z dependence of the bremsstrahlung cross section over the upper portion of the spectrum by using a wide range of target elements, and found that the amount of radiation produced was proportional to the square of the atomic number as given by the Bethe-Heitler theory. The accuracy of the experimental results, however, was not indicated.

It appeared desirable to obtain information on the efficiency of bremsstrahlung production and the angular distribution of radiation intensities in the neighborhood of 20 Mev, where a larger fraction of the electron energy loss is due to radiation. Experiments were performed in which the bremsstrahlung was produced by an external electron beam from the 22-Mev betatron[13] at the University of Illinois. Measurements on the Z dependence of the bremsstrahlung cross section will be discussed in Part I, while experiments on the angular distribution of radiation from a number of targets will be presented in Part II.

I. Z DEPENDENCE OF BREMSSTRAHLUNG PRODUCTION

A. Theory

Bethe and Heitler[3] have calculated the cross section for the production of bremsstrahlung by relativistic electrons impinging both on an unshielded nucleus and on a nucleus whose field is screened by the orbital electrons of the atom. The bremsstrahlung cross section, $\phi(h\nu)$, is the integral of the differential cross section over all possible directions which the electron may have after radiating, and over all possible directions of the quanta emitted in a given energy interval. The calculations of Bethe and Heitler are based on the Born approximation, the condition of validity of which is $Z/137\ll 1$, if the initial and final electron velocities approach c. Thus, it is by no means certain that this calculation is valid for high-Z elements.

For the case of the unshielded nucleus, Bethe and Heitler found that the cross section for bremsstrahlung production depends on the square of the atomic number. However, the cross section for the shielded nucleus in general does not have a simple Z dependence. The effect of screening by the orbital electrons is to decrease the cross section for the production of low energy relative to high energy quanta. Figure 1 gives the theoretical bremsstrahlung spectra for Be and Au as well as for an unscreened nucleus to be expected from monokinetic electrons of 16.93 Mev. An experimental determination of the bremsstrahlung spectrum from a thin platinum target has been made by Koch and Carter,[14] who found overall agreement with the Bethe-Heitler theory.

In the experiments discussed in Sec. IB, wide-angle detectors were used which had a threshold energy high enough that the difference, between the unscreened and screened cases, of the product of detector sensitivity and number of quanta was only a few percent.

Since the energy sensitivity of the threshold detector used in these experiments is known, the theoretically predicted Z dependence of the bremsstrahlung cross section for a screened nucleus can be compared with the experimental measurements. If the corrections for screening are sufficiently accurate, the experimental results may be adjusted to give the Z dependence of the bremsstrahlung cross section for the bare nucleus.

In addition to the radiation considered above, there is the radiation emitted from the collisions of the incident electrons with the orbital electrons of an atom. Heitler[15] has shown by means of the Weizsacker-Williams semiclassical method of calculating cross sections that the radiation emitted in the collision of two electrons (see Fig. 1) is slightly less than, but has a spectrum similar to, that emitted in a collision of an electron with a nucleus of $Z=1$. Thus, since there are Z orbital electrons for each nucleus, one would expect that the Z dependence of the cross section would be approximately Z^2+gZ for low Z, where g is a numerical factor less than unity, whose value depends on the energy sensitivity of the detector.

The threshold detectors which were used in all of the experiments discussed in Sec. IB were copper foils, in

[12] Korsunsky, Walther, Ivanov, Zypkin, and Ganenko, J. Phys. (U.S.S.R.) **7**, 129 (1943).
[13] D. W. Kerst, Rev. Sci. Instr. **13**, 387 (1942).
[14] H. W. Koch and R. E. Carter, Phys. Rev. **77**, 165 (1950).
[15] W. Heitler, *The Quantum Theory of Radiation* (Oxford University Press, London, 1944), second edition, p. 266.

which the radioactivity induced by the nuclear reaction $Cu^{63}(\gamma,n)Cu^{62}$ was measured. The threshold of this reaction is 10.9 Mev.[16] The average energy of the quanta which activated the copper, assuming the bremsstrahlung spectrum of Bethe and Heitler and the measured[17,18] cross section for the (γ,n) reaction of Cu^{63}, was calculated to be 14.3 Mev for a bremsstrahlung spectrum with a peak energy of 16.93 Mev.

The experiments of Sec. IB give information about the production of high energy quanta. The experiments to be discussed in Sec. IC are concerned with the total energy loss of electrons due to radiation. The cross section for this energy loss is obtained by integrating the intensity, $h\nu\phi(h\nu)$ (see Fig. 1), over the complete energy range, and is given by Heitler[15] as

$$U=E_0\phi_{\text{rad}}=\int_0^{h\nu_{\max}} h\nu\phi(h\nu)d(h\nu). \quad (1)$$

This total radiation energy loss can be measured fairly directly by the use of ionization chambers, which are sensitive to the total energy incident on them, and whose sensitivity is nearly independent of the energy of the incident quanta.

The primary purpose of the experiments discussed in Sec. IC, as in IB, was to obtain relative rather than absolute cross sections. However, the measurements in Sec. IC were such that some rough absolute values for the cross section for radiation energy loss could be obtained.

B. Cross Section for Upper Portion of Spectrum

For these experiments, the electrons were removed from the betatron by means of a peeler.[19] They were then focused by means of a magnetic lens while passing through an evacuated cylindrical tube which was connected directly to the evacuated donut (see Fig. 2). The focal length of the lens used for these experiments was about 125 cm. Since the electrons, upon leaving the betatron, have a single energy, they can be focused to form a very small image, the size of which is of the order of a few square millimeters.

Just before emerging from the evacuated tube, the electrons passed through a low pressure, cylindrical ion chamber, which served as a monitor for the electron beam current. The ionization current was amplified and kept constant by the betatron operator during an irradiation. To keep multiple scattering of the beam electrons to a minimum, very thin windows were used on the ion chamber. The window between the vacuum system and the ion chamber was made of 0.6 mg/cm^2 rubber hydrochloride, which can support a maximum air pressure of about 10 cm of mercury. The exit window consisted of 5.21 mg/cm^2 of Cellophane. The air pressure in the ion chamber was kept at approximately 3 mm of mercury. This ion chamber was calibrated by means of a thick-walled aluminum faraday cage connected to a vibrating reed electrometer. The beam current used in these experiments was about 3×10^{-9} ampere.

The method of electron energy control used was that described by Baldwin and Koch[16] and by others.[20] The energy of the electrons is proportional to the setting of an integrator circuit. In the following experiments, the integrator was calibrated by means of the $Cu^{63}(\gamma,n)$ reaction, which has a threshold of 10.9 Mev.

1. X-Ray Beam With Primary Electrons

In the first technique used to measure the Z dependence of the bremsstrahlung cross section, the x-ray beam was not cleared of electrons. Therefore, the threshold detector was activated by both x-rays and the primary electrons. In the second technique, the primary electrons were removed from the x-ray beam. The first, which was used for two pairs of elements, will be discussed briefly.[21]

Two stacks of seven thin foils each, one composed of copper and the other of alternate copper and gold foils, were irradiated with electrons in the target position shown in Fig. 2. (For this method, the magnetic shield, the final deflecting magnet, and the detector foil shown in Fig. 2 were not used.) The two stacks were irradiated in a holder mounted on a synchronous motor in such a way that alternate electron bursts from the betatron activated the two stacks successively. The motor was operated from the frequency tripler of the betatron power supply, so that the motor and the betatron had a fixed phase relationship. This method insured that

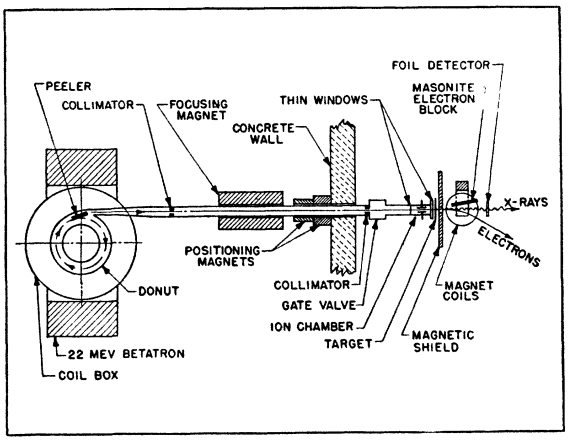

FIG. 2. Schematic drawing (top view) of betatron, focusing magnet, ion chamber, deflecting magnet, and detector position.

[16] G. C. Baldwin and H. W. Koch, Phys. Rev. **67**, 1 (1945).
[17] Johns, Katz, Douglas, and Haslam, Phys. Rev. **80**, 1062 (1950).
[18] B. C. Diven and G. M. Almy, Phys. Rev. **80**, 407 (1950).
[19] Skaggs, Almy, Kerst, and Lanzl, Phys. Rev. **70**, 95 (1946); Radiology **48**, 215 (1948).
[20] McElhinney, Hanson, Becker, Duffield, and Diven, Phys. Rev. **75**, 542 (1949); Katz, McNamara, Forsyth, Haslam, and Johns, Can. J. Research **A28**, 113 (1950).
[21] See L. H. Lanzl, Ph.D. thesis, University of Illinois (1951), for more complete discussion.

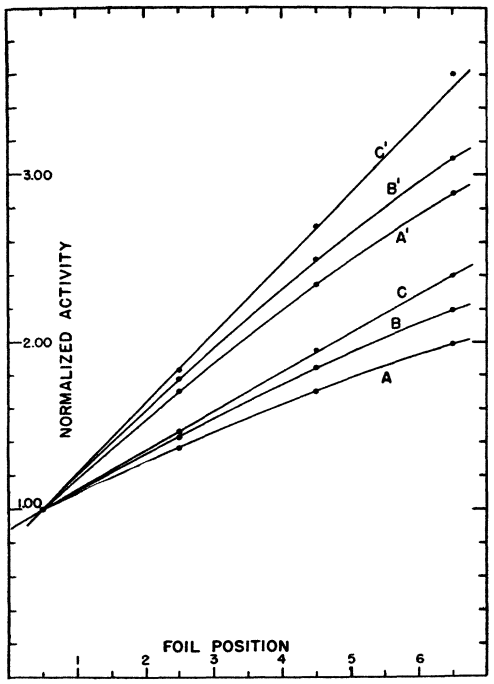

FIG. 3. Normalized activities in Cu−Cu and Cu−Au stacks *vs* foil position for 16.18-Mev electrons. Upper set of curves: Cu−Au stack. Lower set of curves: Cu−Cu stack. A, A': Normalized activity. B, B': Curves A, A' corrected for decrease in electrodisintegration cross section with electron energy. C, C': Curves B, B' corrected for decrease of peak photon energy caused by energy loss of electrons. Foil thicknesses: 46.58 mg/cm² (Cu); 52.35 mg/cm² (Au). Each stack contained 7 foils.

the two foil stacks were irradiated with the same electron beam current.

After irradiation, the activities induced in the four odd-position copper detector foils of each stack were measured by means of an array of Geiger-Müller counters. These activities were then plotted as a function of foil position, giving nearly linear curves[22] after corrections for electron energy loss in the foil stacks had been applied. Corrections are necessary to account for the fact that the electrodisintegration cross section and the peak energy of the bremsstrahlung spectrum produced decrease with decreasing electron energy as the electrons traverse a foil stack, since both of these effects cause a decrease in the induced activity. Using the ratio of slopes of the activity curves, one obtains the ratio of the bremsstrahlung cross sections of gold and copper. Figure 3 shows the activity curves obtained for 16.18-Mev electrons, with the corrections which were applied, for the Cu−Cu and Cu−Au stacks.

This experiment gave a bremsstrahlung cross section ratio for gold to copper of 7.15 ±1.0 percent. This result is to be compared with the cross-section ratio as calculated from the Bethe-Heitler theory for a copper detector. The theoretical ratio is 7.28 for $g=0$ (g is defined in Section A), and 7.13 for $g=1$. It is to be noted that these calculated values differ from the simple Z^2 ratio by only 2 percent. In an early report on this method,[23] some preliminary results were given for which the energy loss corrections had been neglected. The ratio of bremsstrahlung cross sections thus found was about 8 percent higher than that obtained when the corrections had been applied.

From a similar measurement, the cross section ratio of aluminum and copper was found to be 0.210 ±1.7 percent. The corresponding theoretical ratios are 0.203 and 0.211, for $g=0$ and 1, respectively.

A modification of this method involved the irradiation of two stacks of thin foils in which the theoretical collision and radiation losses had been made equal. One stack consisted of copper and the other, of gold and aluminum foils. The radiation produced was detected by a copper foil placed behind each stack. The bremsstrahlung cross section ratio of gold to copper was found using the measurement of the Al−Cu ratio given above. The experimental value thus obtained was 7.21 ±1.2 percent. For this experiment, the kinetic energy of the electrons was 17.98 Mev. At this energy, the theoretical values are 7.25 and 7.10 for $g=0$ and 1, respectively.

For this latter method, the corrections for the degradation of the primary electron energy amounted to only 0.7 percent since the energy losses in the two stacks had been closely matched.

2. X-Ray Beam Free of Primary Electrons

(*a*) *Apparatus and Procedure.*—Figure 2 shows schematically the experimental setup for the technique using an electron-free x-ray beam.[24] The radiators were placed as close as possible to the exit window of the ion chamber. They were supported in a holder which was guided by ways rigidly fastened to a 1 in.-thick iron magnetic shield. The purpose of this shield was to avoid deflecting the beam electrons before they passed through the target.

An electromagnet with wedge-shaped poles which subtended a half-angle of 10° at the target provided the magnetic field. In the vertical direction, the two poles would intercept the few electrons which underwent large angle scattering. In the horizontal direction, an electron block, consisting of masonite, was used for the same purpose, absorbing electrons scattered at angles greater than 10° as measured from the target position. Thus, scattered primary electrons were kept from reaching the detector.

The detector foils were accurately cut circular sheets, 3 in. in diameter, 0.005 in. thick. These were paired and selected so that the weight of any pair differed by no more than 0.15 percent from the mean weight. During irradiation, the detectors were held in place by means

[22] Skaggs, Laughlin, Hanson, and Orlin, Phys. Rev. **73**, 420 (1948).

[23] Lanzl, Laughlin, and Skaggs, Phys. Rev. **74**, 1261 (1948).

[24] Some results obtained by this method were reported recently: L. H. Lanzl and A. O. Hanson, Phys. Rev. **81**, 309 (1951).

of a foil holder mounted rigidly on the magnet base. The center of the holder, which corresponded to the center of the detector, was adjusted to be on the axis of the x-ray beam. The alignment of the holder was checked radiographically. The detector subtended a half-angle of 5.7° at the target position.

During each irradiation, two detector foils were exposed, one being placed directly behind the other. The activated foils were counted simultaneously, being mounted above and below a Geiger-Müller counter, in a cylindrical holder whose axis coincided with the central wire of the counter. During irradiation, the detector foils were held flat and perpendicular to the beam; during the counting period, the foils were bent so as to lie in complete contact with the inner surface of the cylindrical holder.

(*b*) *Measurements and Results.*—Two sets of radiator thicknesses were used. Within each set, the quantity $N(Z^2+Z)$, where N is the number of atoms per cm², and $Z=4$, 13, 29, 47, 79, was made approximately the same for each target. Between sets, $N(Z^2+Z)$ differed by a factor of 2 for each element. Except for the Be, the targets were cut by a 1 in.$\times\frac{3}{4}$ in. die. The Be had been obtained in the form used for the experiments.

Since the beam electrons lose energy, due to ionization and radiation, as they penetrate a target, an appropriate correction has to be applied to the measured activity. For this purpose, the activity induced in a detector as a function of the energy of the incident electrons must be known. This relation was determined

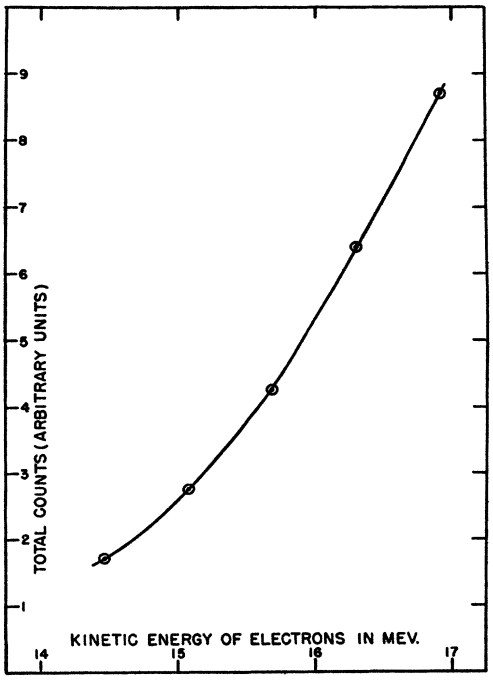

FIG. 4. Activity in copper detector, induced by x-rays from gold radiator, *vs* energy of incident electrons. Target: 37.28 mg/cm² of Au.

TABLE I. Results of experiment on bremsstrahlung production as a function of Z. Incident electron energy = 16.93 Mev.

Element	Thickness (mg/cm²)	Incident energy minus ½ ionization energy loss = average energy (Mev)	Average net activity (original data)	$\frac{Y^a}{N(Z^2+0.75Z)}$ normalized to Au	Theory (Bethe-Heitler) ϕ/Z^2 normalized to Au
Thin series					
Be	257.0	16.69	3921	1.042±0.9%	1.046
Al	84.11	16.85	4266	1.021±1.9%	1.033
Cu	41.00	16.90	4338	1.016±0.5%	1.021
Ag	29.26	16.91	4748	1.020±1.3%	1.011
Au	18.31	16.92	4554	1.000±0.7%	1.000
Thick series					
Be	491.3	16.47	6128	1.045±0.5%	1.046
Al	168.2	16.77	7546	1.031±0.5%	1.033
Cu	90.91	16.85	8465	1.022±0.8%	1.021
Ag	54.52	16.89	8036	1.019±1.2%	1.011
Au	37.28	16.90	8353	1.000±0.5%	1.000

[a] Y is the activity corrected for energy loss of electrons and fraction of radiation intercepted by detector.

(Fig. 4) by irradiating one of the thin gold targets at various electron energies and measuring the activity induced in a pair of detector foils. In this gold target, the ionization energy loss is practically negligible, namely 0.050 Mev for 16.93-Mev electrons. The activity of the detector in this geometry increases slightly faster than the function $(E-E_{th})^3$, where E_{th} is the threshold energy, 10.9 Mev, of the copper detector. The activities in this and in all the other irradiations under this method were normalized to the same electron beam current.

A background count, induced in a pair of detectors when the betatron was run without a target, i.e., when radiation was produced by the electrons in the exit window and in the intervening air, was measured and later subtracted from the counts obtained with targets.

To determine the fraction of the radiation produced in the targets which passed through the detector foils, measurements of the angular distribution of intensities were made, using copper detectors. These measurements indicated that 82 percent of the radiation from the series of thick targets was intercepted by the detector. The measurements on Be and Au appear in Fig. 12. It may be noted here that, in doubling $N(Z^2+Z)$, the relative total induced activity was increased by a factor of 1.9 rather than 2, the difference being due to additional radiation bypassing the detector in the case of the thicker series.

The irradiation times for this experiment were 6 minutes each, and the counting periods, 8 minutes. Including the background measurements, a total of 64 irradiations was made and the activities measured. The average original data for the thick and thin targets, corrected for the air and window background, and also

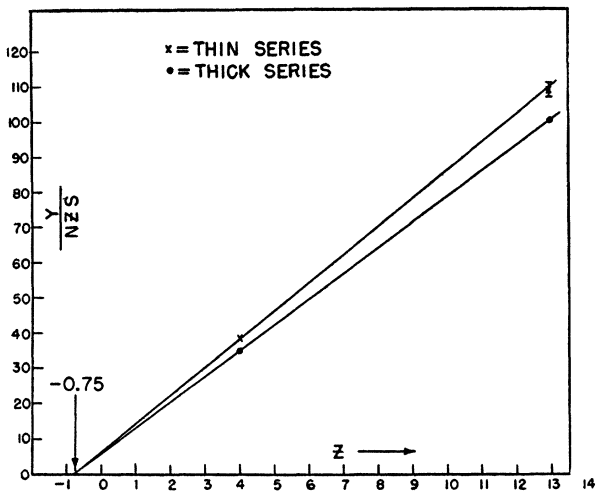

FIG. 5. Graph of relative activity divided by NZS, vs Z, for thin and thick series. The intercept with the Z axis gives the value of $g=0.75$.

the values of the thicknesses of the targets are presented in Table I.

(c) *Analysis of Results.*—The measured activities were corrected for electron energy loss by means of the experimentally determined relation (Fig. 4) between induced activity and electron energy. Each activity was increased by the ratio of the activity at the incident electron energy, 16.93 Mev, to the activity at the average energy of the electrons in the target, this ratio being obtained from Fig. 4. For each target, the average energy used was the incident energy reduced by one-half that lost by ionization.

A further correction of the measured activities was made for slight variations in the fraction of the total radiation intercepted by the detector, from each target within a series. Figure 11 shows that the angular distribution of radiation for the thick Be foil very nearly matched that of the thick Au foil. Therefore, the fractional amount of radiation intercepted by the detector was considered to be the same, and no correction was applied. The $N(Z^2+Z)$ value for the thick Be foil was 10 percent less than that of the thick Au foil. Corrections were made for the other targets by interpolating between Be and Au. However, since the $N(Z^2+Z)$ values of these targets were fairly well matched, these corrections were small, their average amounting to 0.5 percent.

It follows from the discussion in Sec. IA that the cross section for bremsstrahlung production can be represented approximately by $NS(Z^2+gZ)$, where S is the screening factor and g, the fractional effectiveness of electron-electron relative to electron-proton radiation. The data of the present experiment can be used to determine g. The corrected activities, divided by SNZ, were plotted as a function of Z. A simple analysis shows that g is given by the intercept of this curve with the Z axis. As shown in Fig. 5, this value was found to be 0.75, with an error of approximately ± 0.05.

This may be compared to a theoretical value of 0.54, as obtained by the relation,

$$g=\frac{\int_{10.9\text{ Mev}}^{16.93\text{ Mev}}\beta_{\mathrm{Cu}}(h\nu)\phi_{e-e}(h\nu)d(h\nu)}{\int_{10.9\text{ Mev}}^{16.93\text{ Mev}}\beta_{\mathrm{Cu}}(h\nu)\phi_{e-p}(h\nu)d(h\nu)},$$

where $\phi_{e-p}(h\nu)$ and $\phi_{e-e}(h\nu)$ are, respectively, the bremsstrahlung cross sections given by Heitler[25] for electron-proton and electron-electron collisions, and $\beta_{\mathrm{Cu}}(h\nu)$ is the photodisintegration cross section for copper.[17,18] The experimental value of g will be used in the subsequent analysis.

The relative activities, divided by $N(Z^2+0.75Z)$, are

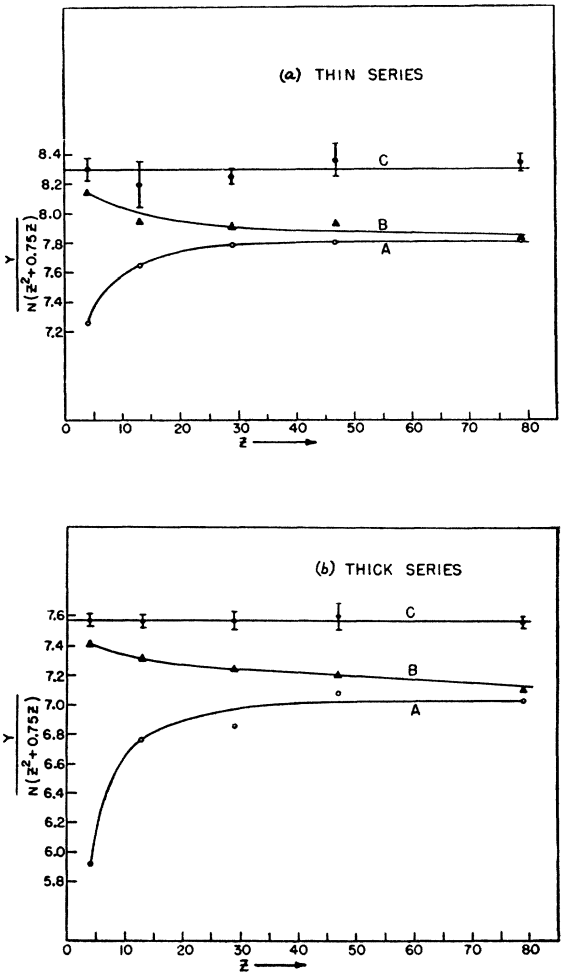

FIG. 6. Graphs of relative activity divided by $N(Z^2+0.75Z)$, vs Z. Curve A: uncorrected activities. Curve B: activities corrected for ionization loss of the electrons in the target and for the fraction of radiation intercepted by the detector. Curve C: adjusted for screening. (a) Thin series; (b) Thick series.

[25] See reference 15, pp. 165, 266.

shown as a function of Z in Figs. 6(a) and 6(b), for the thin and thick target series, respectively. The points on curve A in each of the figures are the uncorrected activities. Curve B, a plot of the corrected activities, gives the variation of the relative bremsstrahlung cross sections as a function of Z, as measured by a copper detector. The corresponding theoretical values, which appear in column 6 of Table I, include the small screening corrections and are calculated for electron-nuclear collisions only. For comparison with the experimental values, they are divided by Z^2 rather than by Z^2+Z.

(d) *Discussion of Results.*—It can be seen from Table I that the experimental results are in very good agreement with the theoretical values when the value of g is taken as 0.75. It should be pointed out that this value will be changed only slightly even if there are large errors in the screening calculations. The remaining variation of curves B indicated in Figs. 6(a) and 6(b) must represent the variation in the Z dependence of the cross section for electron-nuclear collisions not accounted for by the Z^2 term.

If one raised the corrected measurements, shown in curves B, by the screening factor, $1/S$, one would obtain values which represent the bremsstrahlung from radiative collisions with unscreened nuclei and electrons. The screening decreases the radiation by 2.1 percent for beryllium and 6.2 percent for gold. The experimental yields, modified in this manner, appear in the upper curves, C, of Figs. 6(a) and 6(b) for the thin and thick target series, respectively. These points lie very close to a line parallel to the abscissa, i.e., a line where the yield varies as $N(Z^2+0.75Z)$, and therefore indicate that the radiation from an unscreened nucleus varies as Z^2 within the experimental error of about 1 percent.

A comparison of the results from both series, adjusted for screening, appears in Fig. 7. The yields were normalized to the gold foil in each series. The solid lines on this graph represent the variation of the expected yield with Z, assuming g values of 0, 0.75, and 1. It can be seen that the shape of the curves is very sensitive to the choice of g.

C. Cross Section for Total Radiative Energy Loss

The measurements with copper detectors, which are sensitive to the upper portion of the bremsstrahlung spectrum, are of value in determining the dependence of the bremsstrahlung cross section on nuclear charge, since the production of high energy quanta is, relatively, little affected by the presence of orbital electrons. In the experiment to be discussed here, a detector whose response is almost independent of the quantum energy was used, thus giving a measurement of the total energy loss of electrons due to radiation, U [Eq. (1)]. It can be seen from Fig. 1 that relatively more low energy quanta are radiated from the lower Z elements. This additional radiated energy appears as an increase in the total radiation loss, which amounts to 10 percent

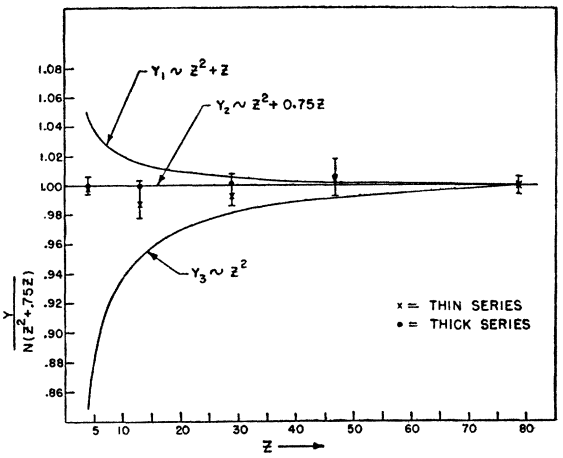

FIG. 7. Graph of $N(Z^2+gZ)/N(Z^2+0.75Z)$ *vs* Z, for $g=0$, 0.75, and 1. The experimental values, normalized to 1 at gold, are also given for the thin and thick series.

for a beryllium as compared to a gold target with the same value of $N(Z^2+Z)$.

Although the primary purpose of these experiments was to investigate the Z dependence of the total radiative energy loss of electrons, it was also possible to obtain rough measurements of the absolute values.

1. Victoreen R Thimble in Aluminum Block

The experimental setup for the absolute radiative energy loss of electrons was nearly the same as that used in the determination of the Z dependence of the bremsstrahlung cross section with copper detectors. As before, the electron beam was deflected magnetically after passing through the target (see Fig. 2). For this experiment, a stack of three copper foils, three inches in diameter, and with a total thickness of 0.1991 g/cm^2, was used as a radiator. The detectors were placed in an aluminum block containing two holes, each of such a size that a 25-roentgen Victoreen thimble could be inserted. During irradiation, one of these holes contained the thimble and the other, a fourth copper disk which was folded in such a way that it subtended very nearly the same solid angle at the target as did the thimble. The holes were aligned with the axis of the x-ray beam, the copper foil occupying the position behind the Victoreen thimble. The thickness of aluminum in front of the detector foil was 5.08 cm, and in front of the thimble, 4.05 cm. The thimble was located 112 cm behind the target, a distance which is great enough that the x-ray beam is considerably wider than the detectors. The thickness of the detector foil was 0.0471 g/cm^2. This was also the thickness of the first and third radiator foils.

Following an irradiation of 20 minutes, the activities of the first and last foils in the target stack, and of the foil in the aluminum block, were counted. The counting geometry was the same as that described in Sec. IB2. The measured counts were corrected for differences in

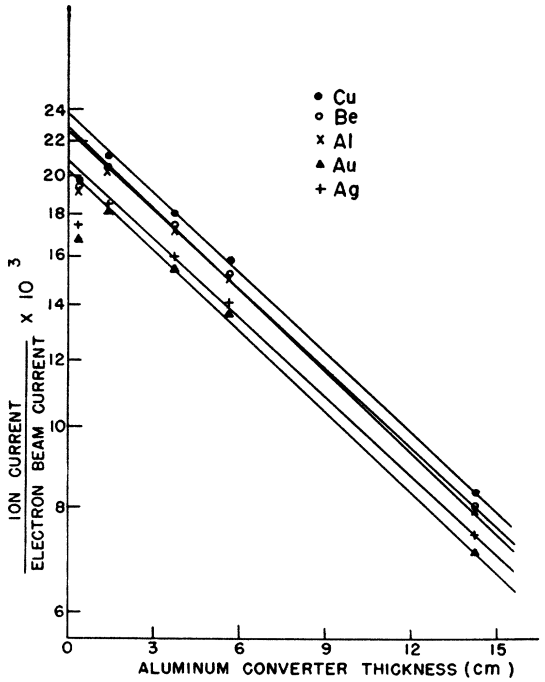

FIG. 8. Ionization current from wide-angle ionization chamber *vs* converter thickness, for five radiators.

the activity distributions on the three foils, and were reduced to the same time interval. The R meter, which had been exposed simultaneously, was read at the end of the irradiation period.

The activity induced in the first foil of the target stack is mainly due to electrodisintegration, whereas that in the last foil is due to the sum of electrodisintegration and photodisintegration activities, the quanta being produced in all three foils. The difference between the activities of the first and third foils is thus a measure of the integrated intensity or total x-ray flux, C_t. The activity per unit area, C_d/A, in the foil placed in the aluminum block is, on the other hand, a measure of the radiation intensity at the R meter.

Since the detector foil was placed at a depth of 5.08 cm within the aluminum block, a correction for absorption of the x-rays had to be applied to the measured activity. In the calculation of the total relative activity due to photodisintegrations produced in the last target foil, several corrections have to be applied. The decrease of the electron energy, and the subsequent decrease of the electrodisintegration cross section, were taken into account. The corrected activities of the first and last copper foils were plotted as a function of foil thickness, at the midpoints of their respective thicknesses. The activity extrapolated to the total thickness of the target, minus the extrapolated zero-thickness activity (electrodisintegration activity), is C_t.

The ratio between the integrated yield, C_t, and the count per unit area for the foil at the position of the R thimble, C_d/A, represents the effective area of the x-ray beam at the position of the R thimble. This ratio, C_tA/C_d, was found to be 327 cm^2. The ratio of the R meter reading in roentgens/min to the saturated activity in counts/min induced in the copper detector, for the particular counting geometry used, is about 3.8×10^{-4} roentgen per count. The total energy radiated can then be obtained from the central yield, Y, as measured by the thimble. Specifically, the total energy radiated is

$$U=(C_tA/C_d)(Y/K),$$

where K is the ionization produced at a depth x in the aluminum by one Mev of bremsstrahlung incident on the surface of the block. K is calculated from the formula,

$$K=\frac{\int_0^{16.93\ \text{Mev}} I(h\nu)\phi(h\nu)\exp(-\mu(h\nu)x)d(h\nu)}{\int_0^{16.93\ \text{Mev}} h\nu\phi(h\nu)d(h\nu)}, \quad (2)$$

where $h\nu$=quantum energy; $I(h\nu)$=ionization in units of ion pairs/cc per quantum/cm^2, as given by Fowler *et al.*;[26] $\phi(h\nu)$=number-of-quanta spectrum (bremsstrahlung cross section; ordinate of Fig. 1 divided by $h\nu$) for copper; x=thickness of aluminum converter; μ=absorption coefficient in cm^{-1} for x-rays in aluminum, where $\mu=\mu_{ph}+\mu_a+\mu_p$ and μ_{ph}=photoelectric absorption coefficient, μ_a=Klein-Nishina (Compton) absorption coefficient, and μ_p=pair production absorption coefficient. The values of these coefficients were taken for the most part from graphs by Evans.[27] K is relatively insensitive to the exact shape of the bremsstrahlung spectrum. At a depth $x=4.05$ cm, K has a value:

$$K=0.633 \text{ ion pair/cm Mev}$$
$$=3.02\times10^{-10} \text{ roentgen cm}^2\text{/Mev}. \quad (3)$$

The yield, Y, as measured by the Victoreen thimble, was 1.11×10^{-3} roentgen per second per 10^{-9} ampere of incident electron current. This gives

$$U=1.20\times10^{9} \text{ Mev/sec per } 10^{-9} \text{ amp.}$$

The theoretical value for copper, based on the Bethe-Heitler theory, was calculated to be 1.33×10^{9} Mev/sec per 10^{-9} amp. The error to be assigned to the Victoreen reading is about 5 percent, and errors of approximately this magnitude may be expected in the measurement of the incident beam current. Thus, the result appears to be in agreement with theory.

[26] Fowler, Lauritsen, and Lauritsen, Revs. Modern Phys. **20**, 236 (1948). J. D. Lawson, A.E.R.E. Report G/R 555, reports a result for K about 4 percent lower than the one used here. The difference is probably smaller than the errors in the calculations.

[27] R. D. Evans and R. O. Evans, Revs. Modern Phys. **20**, 305 (1948).

2. Wide-Angle Ionization Chamber

(*a*) *Experimental Apparatus and Procedure.*—The apparatus used in this experiment was the same as the foregoing, with the exception that the detector was a thick-walled ionization chamber, with a flat, air-filled cylindrical cavity 10.2 cm in diameter and 0.389 cm deep. The axis of the cylinder was aligned radiographically with the axis of the x-ray beam. The chamber was completely surrounded by grade 2S aluminum. The aluminum converter thickness was varied in the course of the experiment. The ionization current was measured with a vibrating reed electrometer. The ion chamber subtended a total angle of 11.6° at the target.

The radiators were the thick series used in the experiment discussed in Sec. IB*2*. The incident kinetic energy of the electrons was again 16.93 Mev.

The yield from this series of targets was also measured by two other ion chambers of smaller diameters, which subtended angles of 1.73° and 0.78°.

(*b*) *Results and Analysis.*—The results of the yield measurements using the 11.6° ion chamber with various thicknesses of an aluminum converter are presented in Fig. 8. The ordinate is the ratio of the detector ion current to the electron beam current, both of which were known by absolute measurements. The abscissa gives the thickness of the converter in cm.

As in the previous measurement of the total radiative energy loss, the ionization, $I(h\nu)$, of Fowler *et al.*,[26] for an air ion chamber with an aluminum converter, was used. Although their calculation was carrried out for a small air cavity ion chamber embedded in a large block of aluminum, upon which a wide, parallel beam was incident, the use of the above ionization function is nevertheless valid, since the ion chamber in this experiment intercepted nearly all of the radiation, and was used to obtain the integral of the intensity over a large fraction of the total radiation.

The constant K of the ion chamber, given by Eq. (2) above, was calculated for Be, Cu, and Au targets, and for a converter thickness of 4 cm. In this calculation, the spectra given in Fig. 1 were used, the nuclear spectrum being weighted by the factor $Z^2/(Z^2+Z)$ and the electron spectrum, by $Z/(Z^2+Z)$. For these three target elements, the value of K was found to be the same within 1 percent. Also, K (for gold) was calculated[28] from Eq. (2) for $t=0$, 1, 2, 8, and 16 cm, as well as for 4 cm. For these converter thicknesses, it was found that K could be very well represented by an exponential function,

$$Kd=1.263\times10^{-19}e^{-\lambda t}d \text{ coulombs/Mev}, \qquad (4)$$

where d=thickness of the air gap of the ion chamber, t=thickness of the aluminum converter, and $\lambda=0.056$ cm^{-1} is the calculated absorption coefficient. This representation is exact for $t=0$ and 1 cm, and differs from the exact value by only 2 percent for a thickness of 16 cm of aluminum.

The fraction of the total energy in the beam intercepted was calculated from the angular distribution of radiation, measured with a small ion chamber, from the gold target of 37.28 mg/cm^2 thickness. The fraction was 0.843.

The yield as measured with the two smaller ion chambers, which subtended angles of 1.73° and 0.78° at the target, gave the same Z dependence for the relative yield as did the larger detector, within the experimental accuracy.

Instead of using the data presented in Fig. 8 for any finite converter thickness in comparing the experimental and theoretical yields, the yield extrapolated to zero thickness (neglecting the smallest converter thicknesses, where equilibrium of radiation and secondary electrons has not yet been reached) was used in connection with Eq. (4) to obtain the radiative energy lost by the electrons as they pass through a target. It is to be noted that the experimental slopes as given in Fig. 8 fit a value of $\lambda=0.07$ rather than the calculated value of 0.056. The absolute cross section as a function of atomic number is presented in Fig. 9, along with the theoretical values times $(Z^2+Z)/Z^2$ as calculated from the Bethe-Heitler theory for electron-nuclear radiative collisions. The ordinate is plotted in terms of $\phi_{\text{rad}}/(Z^2+Z)$, where ϕ_{rad} is the cross section for the total radiative energy loss, as given earlier, and has the dimensions of cm^2.

The curve indicates that the measured absolute cross section is about 10 percent lower than theory for gold. The experimental errors are estimated to be of the order of 10 percent. The discrepancy is probably due to the measurement of the electron beam current and to the ion chamber response.

The variation of the experimental cross section with Z is expected to be more reliable than the absolute values. It can be seen in Fig. 9 that relatively more energy is radiated from low Z materials than is pre-

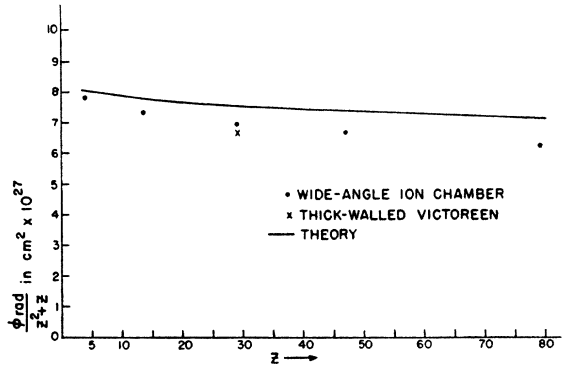

FIG. 9. Cross section, ϕ_{rad}, for radiative energy loss by electrons, divided by (Z^2+Z), *vs* Z. Solid line is calculated from Bethe-Heitler theory. (Z^2 replaced by Z^2+Z in formula for electron-nuclear interactions.) Experimental results are from measurements using ionization chambers.

[28] This calculation was carried out by D. Schiff.

dicted by theory, for foils of the same $N(Z^2+Z)$ value. This discrepancy amounts to about 10 percent between beryllium and gold.

D. Summary

The experimental results on the Z dependence of bremsstrahlung cross sections with a threshold detector and an ion chamber can be summarized as follows:

1. The radiation cross section for the unshielded nucleus is proportional to Z^2 to within 1 percent for the upper portion of a spectrum having a maximum energy of 16.93 Mev. This is in agreement with the theory based on the Born approximation.

2. Electron-electron collisions are found to give 0.75 times the radiation, in the high energy region, expected for electron-proton collisions. The value calculated for this number from theory is 0.54.

3. Rough measurements of the absolute yields of x-rays are in agreement with the Bethe-Heitler theory. There is, however, an indication that the relative yield from a gold target with the same $N(Z^2+Z)$ is somewhat less than that from low Z elements. It is possible that the discrepancy may be accounted for by improved corrections for screening and more accurate consideration of the radiation produced by electron-electron impacts.

II. ANGULAR DISTRIBUTION OF RADIATION FROM FAST ELECTRONS

A. Theory

Measurements were made to determine the angular distribution of radiation emitted at small angles with respect to the direction of the primary electron beam, from targets of various thicknesses. Besides being of intrinsic interest, the angular distribution of radiation is important in many experiments, especially in those for which some knowledge of the total amount of radiation in a given beam is desired.

Stearns[29] and Hough[30] have derived expressions concerning the angular distributions of radiation from fast electrons in a single radiative collision. However, these calculations are not directly applicable in the energy region and the range of angles, respectively, used in the experiments to be discussed here. L. I. Schiff[31] has recently given the following formula for the intrinsic bremsstrahlung intensity at small angles about the direction of the incident electron beam:

$$\sigma(K,x)dKdx=\frac{4Z^2}{137}\left(\frac{e^2}{mc^2}\right)^2\frac{dK}{K}xdx\left\{\frac{16x^2E}{(x^2+1)^4E_0}-\frac{(E_0+E)^2}{(x^2+1)^2E_0^2}+\left[\frac{E_0^2+E^2}{(x^2+1)^2E_0^2}-\frac{4x^2E}{(x^2+1)^4E_0}\right]\ln M(x)\right\},$$

where

$$\mu=mc^2,\quad K=h\nu=E_0-E,\quad x=E_0\theta_0/\mu,$$

$$\frac{1}{M(x)}=\left(\frac{\mu K}{2E_0E}\right)^2+\left(\frac{Z^{\frac{1}{3}}}{111(1+x^2)}\right)^2.$$

For the present work the angular distribution was represented by a simpler expression which does not take into account the variation of the angular distribution with the energy of the radiation, namely,

$$F(\theta_0)=1/[1+(E_0\theta_0/\mu)^2]^2. \tag{5}$$

The fact that the average intrinsic angular distribution is fairly well represented by Eq. (5) will be seen from data using a thin target, which will be presented in the next section.

In an actual experiment, however, either a foil or a volume of gas is employed, so that the angular distribution of the resulting quanta is modified by the multiple scattering of electrons in the target material before radiation takes place. The effect of a large number of target nuclei is to increase the width of the radiation beam over that produced by an infinitely thin foil. Lawson[32] and Schiff[33] have derived expressions for the ratio of the radiation intensity per unit solid angle at an angle θ to the intensity at $\theta=0$. Schiff's calculation uses the theory of multiple scattering developed by Williams,[34] whereas Lawson's calculation uses the theory of Rossi and Greisen.[35]

The experimentally observed x-ray beam widths are somewhat narrower than those calculated using either of the two formulations of the theory mentioned above. This disagreement is consistent with the observation that the multiple scattering widths used in these theories are too large.[36] Baldwin *et al.*[37] have also reported narrower widths for high Z elements with 70-Mev x-rays.

In order to calculate the expected x-ray beam widths more easily than is possible with the form of Eq. (5), the above angle factor was represented by the sum of two gaussian distributions, with constants chosen graphically:

$$1/[1+(E_0\theta/\mu)^2]^2\leqq 0.85\exp[-(E_0\theta/\mu\theta_1)^2]+0.15\exp[-(E_0\theta/\mu\theta_2)^2],$$

with $\theta_1^2=0.553$ rad^2 and $\theta_2^2=2.85$ rad^2. The greatest deviation from Eq. (5), over the range of angles from 0° to 10°, amounts to less than 5 percent.

To obtain an expression for the angular distribution of the x-ray beam from the above expressions, it is necessary to consider the multiple scattering distribution at any depth t. Experiments on multiple scattering of electrons[36] in gold are in good agreement with

[29] M. Stearns, Phys. Rev. **76**, 836 (1949).
[30] P. V. C. Hough, Phys. Rev. **74**, 80 (1948).
[31] L. I. Schiff, Phys. Rev. **83**, 252 (1951).
[32] J. D. Lawson, Proc. Phys. Soc. **A63**, 653 (1950).
[33] L. I. Schiff, Phys. Rev. **70**, 87 (1946).
[34] E. J. Williams, Phys. Rev. **58**, 292 (1940).
[35] B. Rossi and K. Greisen, Revs. Modern Phys. **13**, 240 (1941).
[36] Lyman, Hanson, Lanzl, and Scott, Phys. Rev. **81**, 309 (1951).
[37] Baldwin, Boley, and Pollock, Phys. Rev. **79**, 210 (1950).

Molière's theory,[38] but give $1/e$ widths 10 percent narrower than predicted by the theories of Williams, Snyder and Scott, and Goudsmit and Saunderson.[39] Molière's expression was approximated by a gaussian function of the form $\exp(-E_0^2\theta^2/ct)$ (E_0 = effective electron energy in the foil), with c chosen to give the same $1/e$ value as the exact expression. The factor c was determined from Molière's theory for gold, which agrees with the experimental measurements; for beryllium, the experimental values were used.

The convolution of the multiple scattering distribution with that for the intrinsic distribution, when integrated over the total target thickness, gives the following form:

$$P(\theta, E_0)=\frac{0.85\theta_1^2\left[-\mathrm{Ei}\left(-\frac{E_0^2\theta^2}{ct+(\mu\theta_1)^2}\right)+\mathrm{Ei}\left(-\frac{E_0^2\theta^2}{(\mu\theta_1)^2}\right)\right]+0.15\theta_2^2\left[-\mathrm{Ei}\left(-\frac{E_0^2\theta^2}{ct+(\mu\theta_2)^2}\right)+\mathrm{Ei}\left(-\frac{E_0^2\theta^2}{(\mu\theta_2)^2}\right)\right]}{0.85\theta_1^2\ln[1+ct/(\mu\theta_1)^2]+0.15\theta_2^2\ln[1+ct/(\mu\theta_2)^2]}, \quad (6)$$

where Ei is the exponential integral function. This expression is similar to that given by Lawson.[32]

Experiments which have been performed using targets such as the standard betatron target or metal wires cannot be compared with theory because the target thickness is not uniform. Measurements on the angular distribution were made by Lawson[32] at 10 Mev, with a thin, uniform gold target, and by Koch and Carter[14] at 19.6 Mev, with a thin platinum target. The angular width found by Lawson is somewhat greater than that given by Schiff's theory, while the measurement of Koch and Carter is in agreement with this theory.

B. Measurements and Procedure

A number of measurements on the angular distribution of radiation were made, using a focused 16.93-Mev electron beam from the betatron. The experimental arrangement was the same as that described earlier, in which an electron-free x-ray beam was used to measure the Z dependence of the cross section for bremsstrahlung production (Fig. 2). Again, the beam, before striking a target, passed through the two thin windows of the ion chamber monitor, and through approximately 2 inches of air, about one inch of this path being in front and one inch behind the target.

Measurements were made on uniform Be and Au targets. For Be, only one target thickness was used, while the thicknesses of gold ranged from 0.7 mil to 600 mils. One of the three types of detectors used was Industrial-A x-ray film, exposed with and without a $1\frac{3}{4}$ inch thick presdwood converter. This film, used because of the linearity of its dose-density curve,[40] was developed in D-19b under standard conditions of developing time, temperature, agitation, and fixing time. During exposure, the film was held in a standard Eastman cardboard cassette containing five mils of lead backing, placed perpendicular to the beam, $15\frac{1}{8}$ inches from the target. Densities were measured by means of a Weston photographic analyzer, calibrated against an Eastman transmission densitometer. The angular resolution, determined by the diameter of the densitometer field, was 0.15°.

A second detector used was a small cylindrical, lead-walled ion chamber of $\frac{1}{2}$ in. inside diameter, $1\frac{1}{2}$ in. inside length, and a wall thickness of $\frac{1}{8}$ in. The ion chamber was placed 30.75 in. behind the target, its axis parallel to the central ray of the x-ray beam, and subtended an angle of 0.9° at the target. Its current was measured with a vibrating reed electrometer. For measuring the current at various angles, the chamber was moved by remote control both horizontally and vertically by means of a pair of Selsyn motors.

A row of copper cylinders, 1 in. in outside diameter and $1\frac{1}{2}$ in. long, with a $\frac{1}{16}$-in. wall, was another type of detector used. These cylinders were placed $51\frac{1}{16}$ in. behind the target with their axes vertical, and set side by side in a straight line perpendicular to the beam axis. By this method, only the horizontal distribution of intensities was measured, with an angular resolution of 1.1°. A number of cylinders was thus irradiated simultaneously, and the induced activities then counted successively with a Geiger counter.

The angular distribution of x-rays from the windows of the ion chamber and the short air path gives a fair measurement of the intrinsic angular distribution. The distributions from the thicker targets, on the other hand, are determined primarily by multiple scattering.

A special run was made in which the small lead-walled ion chamber was held in a fixed position along the central ray of the x-ray beam, and the yields from the various gold foils were measured. An analysis of these data is given in Sec. IID.

A series of measurements was made in which wide-angle copper detectors were used to find the relative amount of radiation produced in various gold targets. One detector subtended an angle of 180° and the other, 11.4° at the target.

C. Results Using Small-Angle Detectors

The angular distribution measurements, made with the small lead ion chamber and with film, on the radiation produced in the monitor windows and in the air traversed by the electrons near the target were in good

[38] G. Molière, Z. Naturforsch. **3a**, 78 (1948).
[39] E. J. Williams, Proc. Roy. Soc. (London) **169**, 531 (1939); S. Goudsmit and J. L. Saunderson, Phys. Rev. **58**, 39 (1940); H. Snyder and W. T. Scott, Phys. Rev. **76**, 220 (1949).
[40] G. D. Adams, Ph.D. thesis, Part II, University of Illinois (1942).

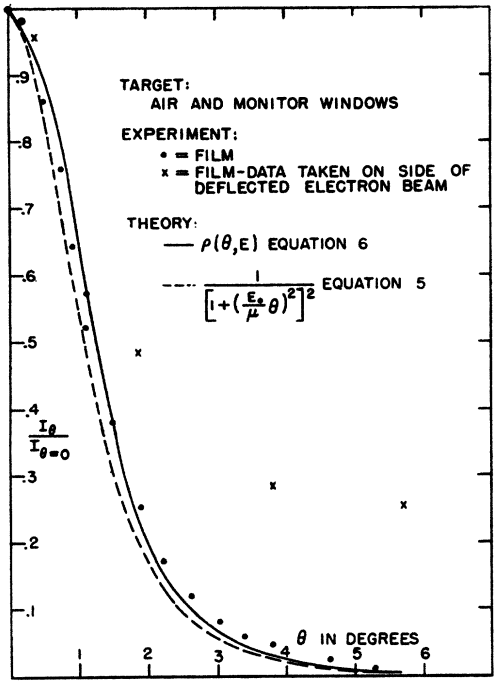

FIG. 10. X-ray intensity, as determined by the net film density, *vs* angle, for monitor windows and air, normalized to 1 at $\theta=0°$. The theoretical intrinsic x-ray distribution, and this distribution modified by multiple scattering, are also given. The crosses are those points measured on the side of the deflected electron beam.

agreement with each other. The increase in the x-ray beam width due to multiple scattering and due to the inherent angular spread of the electron beam over the width of a parallel, unscattered electron beam is small. Therefore, the measurements made can be used to check Schiff's formula for the intrinsic x-ray beam width, Eq. (5). Figure 10 is a plot of film density *vs* angle, with the peak density normalized to unity. Equations (5) and (6), for electrons of kinetic energy equal to 16.93 Mev (E_0 is the total energy of the electrons), are shown in this figure. From Molière's theory, the $1/e$ width of multiple scattering was calculated for the windows and the air. Under the assumption that the multiple scattering and primary electron beam shapes are gaussian, an assumption which is reasonable because its overall effect is small, the squares of the $1/e$ angles of these two distributions were added, the square root of their sum giving the $1/e$ width of the combined gaussian function. It was this combined distribution which was used in Eq. (6) for the theoretical curve in Fig. 10. Although the plot of Eq. (6) does not quite pass through the experimental points at the lower end of the distribution, the shape of a curve drawn through these points indicates that the intrinsic width may be represented by Eq. (5). A better fit to the experimental data in Fig. 10 would be obtained if an approximation to Schiff's intrinsic distribution were used which is more accurate than the two gaussian functions.

For the film data, the angular distribution of radiation was the same in the two vertical directions from the beam center, and in the horizontal direction opposite to that in which the electrons were deflected. On the side of the electrons, the film measurements indicated an asymmetric distribution, due to electrons which radiated while being deflected by the magnet. The crosses in Fig. 10 show this effect. The asymmetry becomes negligible for the thicker foils. The ion chamber measurements were in complete agreement with the film measurements for the radiation from the air and the monitor windows.

The fog density in the film measurements, for all targets, was between 0.18 and 0.21. It was this background which was subtracted to obtain the net density. The maximum density for all films measured ranged from 0.5 to 3.0; for each target, at least two exposures were made whose peak densities differed by about two. This was done in order to check the linearity of the film response.

Some of the data obtained using ion chamber and copper detectors are plotted in Figs. 11 to 13. The thicknesses of the gold targets, as well as the detectors used, are indicated on these graphs. The theoretical curves were calculated by means of Eq. (6), in which gaussian distributions for the multiple scattering were used whose $1/e$ angles were those calculated from Molière's theory for gold, modified to account for multiple scattering in the windows and air, and for the primary electron beam width. The electron energy used in these calculations was the incident energy of 16.93 Mev, reduced by one half the ionization loss as calculated from Heitler's[41] formula. Since the Molière theory of multiple scattering cannot be represented in its entirety without appropriate tables, the resulting $1/e$ widths for the gold foils are given in Table II. For the beryllium foil, the experimental $1/e$ width for multiple scattering, obtained from scattering chamber measurements,[36] was used for the distribution of radiation.

The theoretical x-ray distributions were not calculated for gold thicknesses greater than 967 mg/cm^2 because x-ray absorption in the target itself begins to become appreciable. In fact, in the experiment on central yields discussed in Sec. IID, it is shown that photon absorption outweighs photon production for

TABLE II. $1/e$ widths of multiple scattering.

Element	Thickness	$(\theta_{1/e})^2$	$(\theta_{1/e})^2$ modified by window and air multiple scattering and divergence of the electron beam	Source of $(\theta_{1/e})$
Be	491.3 mg/cm^2	15.60 deg^2	16.38 deg^2	Expt. Molière
Au	37.28 mg/cm^2	12.62 deg^2	13.40 deg^2	Expt. Molière
Au	51.5 mg/cm^2	18.55 deg^2	19.32 deg^2	Expt. Molière
Au	247.1 mg/cm^2	101.16 deg^2	101.94 deg^2	Expt. Molière
Au	967.0 mg/cm^2	563.78 deg^2	564.56 deg^2	Expt. Molière

[41] See reference (15), p. 217.

gold foils thicker than 1700 mg/cm², for 16.93-Mev electrons.

Figure 11 shows a comparison of the measurement on the angular distribution of x-rays from 491.3 mg/cm² of beryllium and 37.28 mg/cm² of gold. These were the thicker targets used in the experiment on the Z dependence of bremsstrahlung [Sec. IB2]. Measurements of the angular distribution using x-ray film were in close agreement with those using copper threshold detectors. Since the film is most sensitive to low energy x-rays, while the copper is sensitive only to high energy quanta, the result indicates that there is no marked energy change with angle for such thin targets. This is not the case for targets of greater thickness. Although the angular distributions for the gold and beryllium targets were very nearly the same, the absolute values of the film densities differed by about a factor of two. More precisely, the maximum film densities minus the fog background density, normalized to the same number of incident electrons (7×10^{11} electrons), were 1.50 and 0.69 for these beryllium and gold targets, respectively. This striking effect can be attributed to the difference in the relative number of low energy quanta from these beryllium and gold targets. The beryllium nucleus is screened less by the orbital electrons and, therefore, should yield more low energy quanta than gold.

Figure 12 is a graph of the angular distribution of radiation from a 51.5 mg/cm² gold target, as measured with film and ion chamber. Besides the experimental data, this figure includes the theoretical angular distribution as given by Schiff.[33] In the derivation of this formula, Schiff used the electron multiple scattering theory by Williams, which gives a distribution wider than that of Molière's theory. The closer agreement of the experiment with Eq. (6) indicates that, at least for high Z, Molière's theory is more accurate than that of Williams. Also, Fig. 12 shows the distribution as given by Lawson's formula, modified in that the multiple scattering gaussian of Rossi and Greisen[35] assumed by him has been replaced with Molière's theory, and the $1/e$ angle of radiation for an infinitely thin foil was made equal to the $1/e$ angle from Schiff's formula, Eq. (5). In Lawson's expression, the radiation width is assumed to be a single gaussian. Equation (6), however, agrees somewhat better with the experimental results.

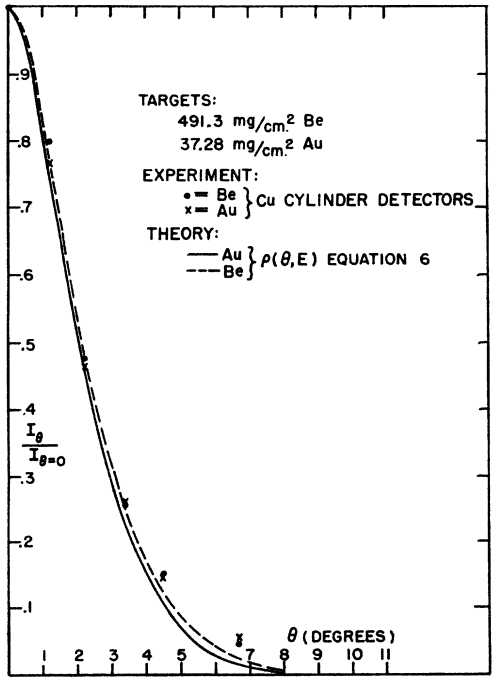

FIG. 11. Angular distribution of radiation from 491.3 mg/cm² Be target and 37.28 mg/cm² Au target, measured with Cu threshold detectors. Theoretical curves from Eq. (6).

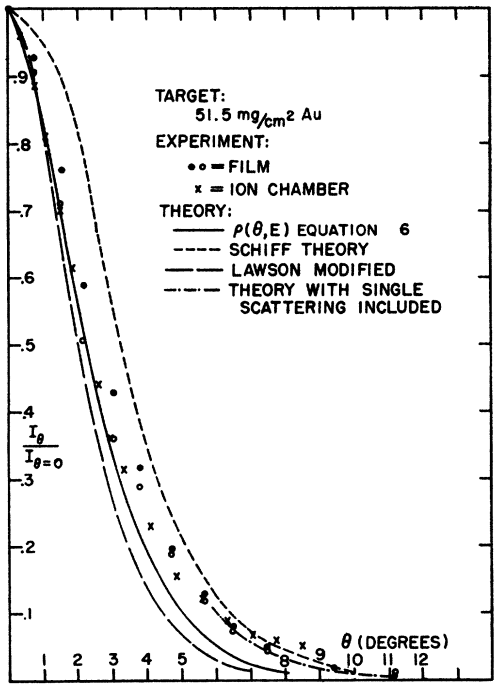

FIG. 12. Angular distribution of radiation from 51.5 mg/cm² Au target, measured with film and ion chamber. Theoretical curves from Eq. (6), Schiff (reference 33) and Lawson (reference 32). Estimate of theory including single scattering of electrons is indicated.

The lack of agreement between the experimental and the theoretical curves at large angles can be explained at least in part by the fact that the gaussian approximation to the electron scattering distribution is definitely poor at large angles. The contribution by electrons which have undergone large-angle scatterings can be estimated by comparing the actual scattering to that accounted for by the gaussian approximation. If one assumes that these electrons make radiative collisions during the remainder of their path in the target, one can estimate the contribution of these electrons to the angular distribution of the x-rays. To a first approximation, this contribution varies as $1/\theta^4$. The

dashed curve in Fig. 12 indicates this calculated contribution due to large-angle scattering. It can be seen that this contribution is the major one not accounted for by the simple form of the theory.

At target thicknesses larger than 100 mg/cm^2 of Au, the distribution as measured with film (thin Pb converter) starts to become wider than that measured with the ion chamber. With successively thicker foils, this difference becomes more pronounced until, at a thickness of 3910 mg/cm^2, agreement between the data from the two detectors is again reached. A possible explanation is that the low energy quanta, to which the film is very sensitive, are absorbed in the target itself for greater target thicknesses.

Figure 13 gives the ion chamber data and the theory for a number of gold thicknesses.

In the ion chamber data, the random errors are estimated to be of the order of 1 percent near the peak.

D. Results of Central Yield Measurements

This section deals with the analysis of the data on central yield as a function of target thickness, as measured with the small lead-walled ion chamber. Lawson[32] gives an expression for the central yield as a function of primary electron energy and target thickness. This expression involves multiple scattering and the beam width expected for radiative collisions. Lawson used Rossi and Greisen's multiple scattering formula and a gaussian distribution for radiative collisions. Instead, an expression approximating Molière's theory of multiple scattering by a gaussian, and the radiative distribution described by two gaussian functions (see Sec. A), is compared with the experimental results. This expression for the central yield per unit solid angle is given by

$$R(E_0, t)=(E_0^2\sigma/c)\{1.102\ln(1+ct/\mu^2\theta_1^2)+\ln(1+ct/\mu^2\theta_2^2)\}, \quad (7)$$

where E_0 is the total energy (inlcuding the rest mass) of the electrons incident on the foil, and where $\theta_1^2=0.553$ rad^2 and $\theta_2^2=2.85$ rad^2, as in Sec. A. This expression is the denominator of Eq. (6), multiplied by the square of the incident electron energy which, in Eq. (6), cancelled with a factor E_0^2 in the numerator. σ is a constant proportional to the radiation loss in the foil ($NE_0\phi_{\text{rad}}$). The factor c is not strictly a constant, but is a slowly varying function of the thickness, as well as of the electron energy. However, since the initial layer of a target contributes more than any subsequent layer to the forward yield, the factor c was determined from Molière's theory for the smallest target thickness used, and regarded to be the same for all thicknesses, for the sake of simplicity of analysis. The thinnest target used in this series was 0.0515 g/cm^2 of gold. The multiple scattering distribution from a target of this thickness is very nearly gaussian to angles well beyond the $1/e$ width. For this target, and an incident electron kinetic energy of 16.93 Mev, the value of c was calculated to be 1.090×10^5 deg^2 Mev^2/(g/cm^2). To summarize, the logical choice of c would be that calculated for a thin foil, since most of the radiation is produced in the initial layer of a target, but not so thin that the multiple scattering from this foil is not adequately represented by a gaussian distribution.

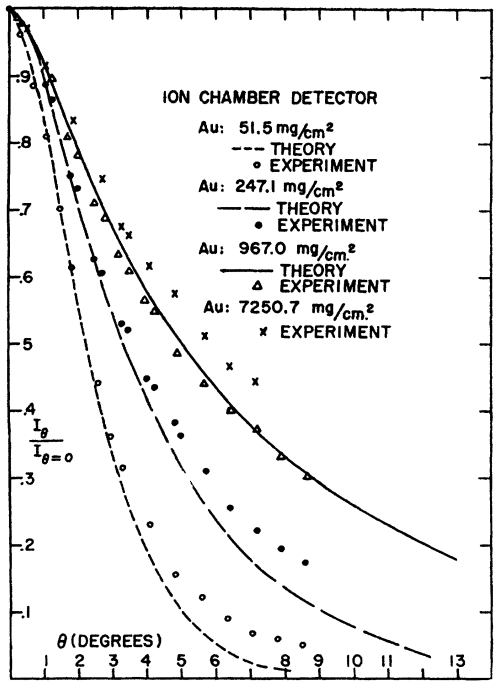

FIG. 13. Angular distribution of radiation for four Au targets, measured with ion chamber. The three corresponding theoretical curves are given, as calculated from Eq. (6).

The rate of change of the central yield with target thickness is given by

$$dR(E_0, t)=\frac{E_0^2\sigma}{c}\left\{1.102\frac{k_1dt}{1+k_1t}+\frac{k_2dt}{1+k_2t}\right\}, \quad (8)$$

where, $k_1=c/\mu^2\theta_1^2$ and $k_2=c/\mu^2\theta_2^2$. This expression, then, gives the amount of radiation produced in a layer of target material between thicknesses t and $t+dt$, for electrons of energy E_0. Now, since, for large target thicknesses, the energy is not constant, but decreases due to radiation and ionization losses, E_0 is a function of the target thickness. Using the formulas of Heitler[41] for radiation and ionization loss in gold, which is very nearly linear in a plot of energy loss *vs* incident energy, one obtains the following expression:

$$E(t)=[(\alpha_0+\beta E_0)e^{-\beta t}-\alpha_0]/\beta, \quad (9)$$

where α_0 is the intercept on the ordinate and β, the slope, in the plot of energy loss per unit thickness *vs* electron energy. For gold, the values of these constants were determined graphically to be

$$\alpha_0=17.8\text{ Mev/cm}=0.921\text{ Mev/g/cm}^2$$

and

$$\beta=3.13\ \text{cm}^{-1}=0.162\ [\text{g/cm}^2]^{-1}.$$

If the electron energy loss is appreciable in a given target, E_0 in Eq. (8) must be replaced by $E(t)$ of Eq. (9).

Introducing Eq. (9) into Eq. (8) and integrating from 0 to t, one obtains the expression for the forward yield from a target of thickness t,

$$R(E_0,t)=\frac{\sigma}{c\beta^2}\Big\{(\alpha_0+\beta E_0)^2\int_0^t e^{-2\beta t}\Big(\frac{1.102k_1}{1+k_1t}+\frac{k_2}{1+k_2t}\Big)dt$$
$$-2\alpha_0(\alpha_0+\beta E_0)\int_0^t e^{-\beta t}\Big(\frac{1.102k_1}{1+k_1t}+\frac{k_2}{1+k_2t}\Big)dt$$
$$+\alpha_0^2\int_0^t\Big(\frac{1.102k_1}{1+k_1t}+\frac{k_2}{1+k_2t}\Big)dt\Big\}. \quad (10)$$

The last of these integrals is easily found to have the value

$$\frac{\sigma\alpha_0^2}{c\beta^2}\{1.102\ln(1+k_1t)+\ln(1+k_2t)\}.$$

In order to evaluate $R(E_0, t)$, the exponential in Eq. (9) was expanded for a value of $\beta t_1\ll 1$. For large target thicknesses, t_n, where βt_n was not necessarily less than 1, the first two integrals of Eq. (10) were evaluated numerically from t_1 to t_n, and the results added to that from 0 to t_1.

Figure 14 is a plot of the relative net yield, i.e., of the net current from the ion chamber, from gold as a function of target thickness. The plot shows that the larger thicknesses were such that photon absorption in the targets became appreciable. For these thicknesses, even though the radiation spectrum is far from being monochromatic, the measured yield falls off exponentially with target thickness. The absorption coefficient, λ, in the factor $e^{-\lambda t}$, was determined experimentally to be 0.0555 $(\text{g/cm}^2)^{-1}$ for gold.

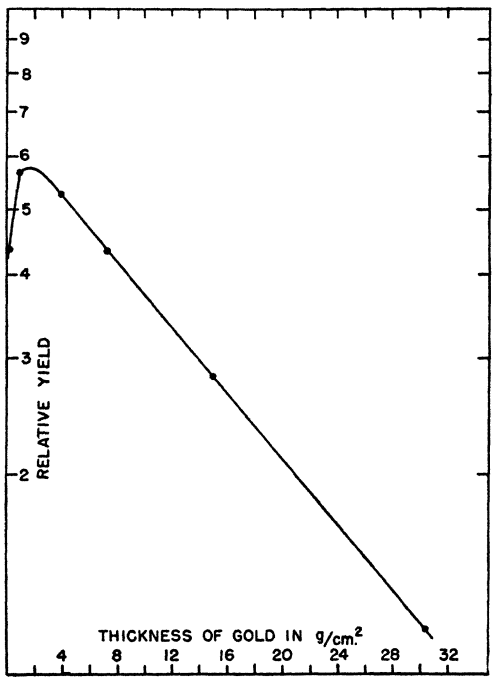

FIG. 14. Experimental measurement of central yield (logarithmic scale) *vs* gold target thickness, for 16.93-Mev electrons.

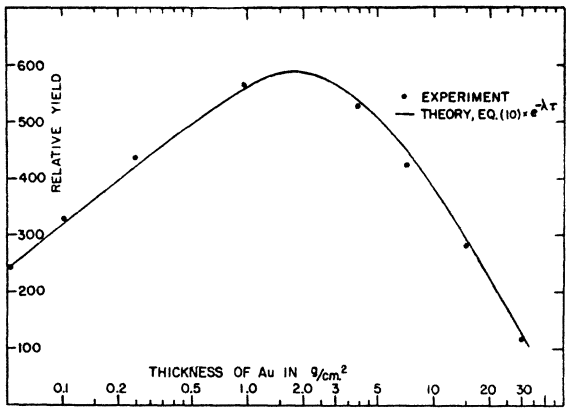

FIG. 15. Comparison of theory and experiment for central yield *vs* target thickness in gold (logarithmic scale). Incident kinetic energy of electrons is 16.93 Mev. $R(E_0, t)e^{-\lambda t}$ is the theoretical expression, where $R(E_0, t)$ is given by Eq. (10) and λ is the effective photon absorption coefficient.

The theoretical expression given by Eq. (10) does not include photon absorption. Therefore, for a comparison of theory and experiment, $R(E_0, t)$ is multiplied by $e^{-\lambda t}$. Equation (10) no longer applies for foil thicknesses such that the energy loss would be more than the incident electron energy. Thus, for target thicknesses greater than the maximum electron range, the thickness equivalent to this range is used in comparing the theoretical expression, including the absorption factor, with experiment. The thickness corresponding to this maximum range for gold, as determined from Eq. (9), was 8.66 g/cm².

The experimental results are plotted in Fig. 15, together with $R(E_0, t)e^{-\lambda t}$ as given by Eq. (10). The values are normalized to the yield of the first foil, of thickness 0.0515 g/cm². The peak yield as determined experimentally occurs at about 1.7 g/cm², while the theoretical peak is at approximately 1.8 g/cm².

The increase in yield for small thicknesses, calculated as described above, appears to be slightly slower than the experimental values indicate; however, the shape of the experimental rise agrees with theory in being proportional to the logarithm of the target thickness.

E. Results Using Wide-Angle Copper Detector

A wide-angle copper threshold detector was used to measure the radiation produced in gold and copper by 16.93-Mev electrons. As in Sec. IB2, the detectors were flat copper disks, 3 inches in diameter. These subtended a total angle of 11.4° at the radiator position.

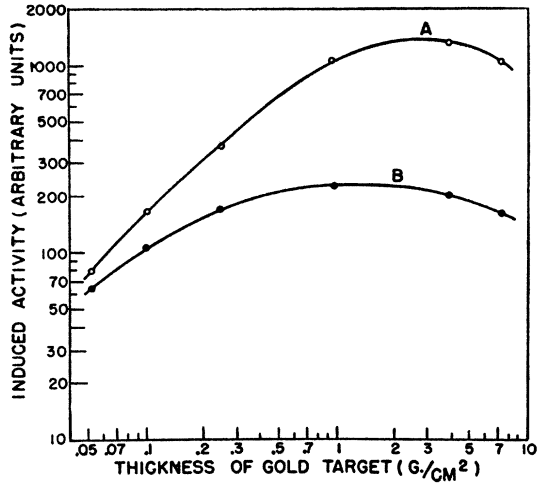

FIG. 16. X-ray induced copper activity from gold targets of various thicknesses. Curve A: detector subtending 180° at target. Curve B: detector subtending 11.4° at target. Electron energy = 16.93 Mev, where effective energy response of detector = 14.3 Mev.

Two series of measurements were made, with the set of gold radiators used for the central yield experiment. In one series, gold foils served as radiators, a copper disk at a distance of $15\frac{1}{8}$ inches behind them being the detector. In the second series, in addition, a copper disk of the same dimensions and weight as the detector disk was placed directly behind the gold foils, and served both as a radiator and a detector. The thickness of the copper disks was 0.1088 g/cm²; the gold target thicknesses ranged from 0.0515 to 7.25 g/cm².

The activities in the two copper foils of the series in which both gold and copper acted as radiators were measured, while the activity in the one detector was measured for the series having only a gold radiator foil. In order to correct for radiation produced in the monitor windows, an irradiation was made without a target foil. Also, to correct the activity, in the copper detector immediately behind the gold, for electrodisintegration and bremsstrahlung activity produced in the detector itself, a measurement was made in which a copper foil alone acted as a target. The irradiations were monitored with the ion chamber mentioned previously. All of the measured activities were reduced to the same counting interval and normalized to the same beam current. The relatively small activity produced in the detectors due to the air and the monitor windows was subtracted.

The activity induced in the copper foil directly behind the gold radiators measured the total radiation, from 0° to 90°, leaving a target. The radiation leaving the target is, of course, not the actual total amount produced, since some absorption takes place. To reduce the activity induced in the total radiation detector to that due to the gold alone, a correction was applied, eliminating the induced activity due to electrodisintegrations and bremsstrahlung produced in the detector. The results of these measurements appear in Fig. 16. No analysis will be given here.

F. Summary

The results of the experiments discussed in this part may be summarized as follows:

1. The experimental measurements on the angular distribution of radiation from a very thin foil were used to check Schiff's expression (see Eq. (5)) for the intrinsic angular distribution of bremsstrahlung and were found to be in good agreement.

2. The angular distributions of radiation from foils of various thicknesses were measured. The results are in agreement with an expression given by Eq. (6) if a correction is applied at large angles for the single scattering tail. This expression differs from those of Schiff[33] and Lawson[32] in that the intrinsic distribution of radiation is taken into account more accurately. A gaussian approximation of Molière's theory of multiple scattering in Eq. (6) agrees more closely with experiment than does the gaussian approximation based on Williams' theory, as used by Schiff.

3. An approximate expression is given for the central yield as a function of target thickness. This expression ($e^{-\lambda t}R(E_0, t)$, where $R(E_0, t)$ is given by Eq. (10) and λ is the photon absorption coefficient) is similar to that of Lawson,[32] with the exception that an improved form of the intrinsic angular distribution of bremsstrahlung and of multiple scattering is used. It includes a different gaussian approximation for the multiple scattering of electrons, and the decrease in primary electron energy in the target material is taken into account. The experiment on central radiation intensities, using a wide range of gold target thicknesses, was found to be in agreement with this calculation.

4. In Sec. E, some measurements on the total intensity of radiation emitted by a target and that intercepted by a wide-angle copper detector as a function of target thickness are presented.

The setting up of the apparatus and the making of measurements were accomplished with the able assistance of Messrs. D. E. Riesen, W. Unruh, D. Schiff, M. B. Scott, and other members of the electron beam group. The authors wish to acknowledge the assistance of E. F. Lanzl in the preparation of the manuscript.